

Positron measurements with the HEAT-pbar instrument

S. Coutu¹, A. S. Beach¹, J. J. Beatty¹, A. Bhattacharyya², C. R. Bower², M. A. DuVernois^{1,*}, A. W. Labrador³, S. P. McKee⁴, S. A. Minnick¹, D. Müller³, J. A. Musser², S.L. Nutter^{1,**}, M. Schubnell⁴, S. P. Swordy³, G. Tarlé⁴, and A. D. Tomasch⁴

¹Department of Physics, The Pennsylvania State University, University Park, PA 16802, USA

²Department of Physics, Indiana University, Bloomington, IN 47405, USA

³Enrico Fermi Institute and Department of Physics, University of Chicago, Chicago, IL 60637, USA

⁴Department of Physics, University of Michigan, Ann Arbor, MI 48109-1120, USA

*Now at the School of Physics and Astronomy, University of Minnesota, Minneapolis, MN 55455, USA

**Now at the Department of Physics and Geology, Northern Kentucky University, Highland Heights, KY 41099, USA

Abstract. The HEAT-pbar magnet spectrometer, flown on a balloon in Spring 2000, was designed for measurements of cosmic-ray antiprotons. However, the use of several particle identification methods also permits the detection of electrons and positrons with high rejection power against protons, pions and muons. We present new measurements of the positron fraction above 5 GeV, which confirm the results of the earlier HEAT-e[±] flights, albeit with an independent technique. In particular, we investigate the region below 10 GeV, which previously had indicated some structure, possibly suggesting a small primary contribution to the positron intensity.

duction (Protheroe 1982, Moskalenko & Strong 1998). However, the results of HEAT-e[±] include a feature that could possibly indicate a small primary positron contribution (Coutu et al. 1999).

We have modified the HEAT instrument to detect antiprotons at energies from 4.5 to 50 GeV in the cosmic-ray flux. This HEAT-pbar instrument was flown from Ft Sumner, NM, in Spring 2000. Details of the instrument and its performance during the flight are given elsewhere (Nutter et al. 2001). The payload comprises a superconducting magnet spectrometer with drift-tube hodoscope (used to measure the magnetic rigidity and charge sign of the particle), a time-of-flight system (used to measure the velocity and direction of travel of the particle, as well as the magnitude of its charge), and an array of proportional chambers with which multiple measurements of dE/dx losses are made (used to identify the particle). A first measurement of the antiproton abundance with this instrument is presented elsewhere (Musser et al. 2001). The array of particle detectors also allows the identification of electrons and positrons. We present here a new measurement of the positron fraction from the Spring 2000 flight of the HEAT-pbar instrument, and discuss the implications of the results.

1 Introduction

Cosmic-ray electrons and positrons constitute an interesting probe of cosmic-ray confinement and source distribution in the Galaxy, providing information that complements what can be learned from the more abundant nucleonic component. The flux of e[±] observed at Earth is dominated by negative electrons from primary acceleration sites. However, about 10% of the total flux are secondary particles (in equal numbers of e⁺ and e⁻), resulting from hadronic interactions of the nuclear cosmic rays with nuclei in the interstellar medium. Measurements of the positron fraction e⁺/(e⁻+e⁺) above 10 GeV made prior to 1995 (Agrinier et al. 1969, Buffington et al. 1975, Müller & Tang 1987, Golden et al. 1987, Golden et al. 1994) had indicated a larger than expected positron content, interpreted variously as the possible signature of new, possibly exotic, antimatter sources (e.g., Kamionkowski & Turner 1991). Newer measurements, including observations with the HEAT-e[±] instrument, have been made in the past few years (Barwick et al. 1995, Golden et al. 1996, Clem et al. 1996, Barbiellini et al. 1996, Barwick et al. 1997). Using more powerful balloon instruments, these newer measurements have indicated a positron fraction distribution in better agreement with models of secondary pro-

2 e[±] Identification

The vertical geomagnetic cutoff rigidity at the latitudes near Ft Sumner preclude the detection of primary particles below about 4 GV. The 2000 flight took place at atmospheric overburdens between 4.5 and 11 g/cm², during a time of some 22 hours.

The time-of-flight (ToF) system measures the velocity of the particle $\beta = v/c$ with a resolution of $\sigma_\beta = 0.09$, permitting complete rejection of upward-going particles; in selecting electrons and positrons, we require $0.85 < \beta < 1.5$. In addition, the amount of light deposited in the scintillation counters of the ToF system is used to measure the magnitude of the particle's electric charge Ze twice (in top and bottom

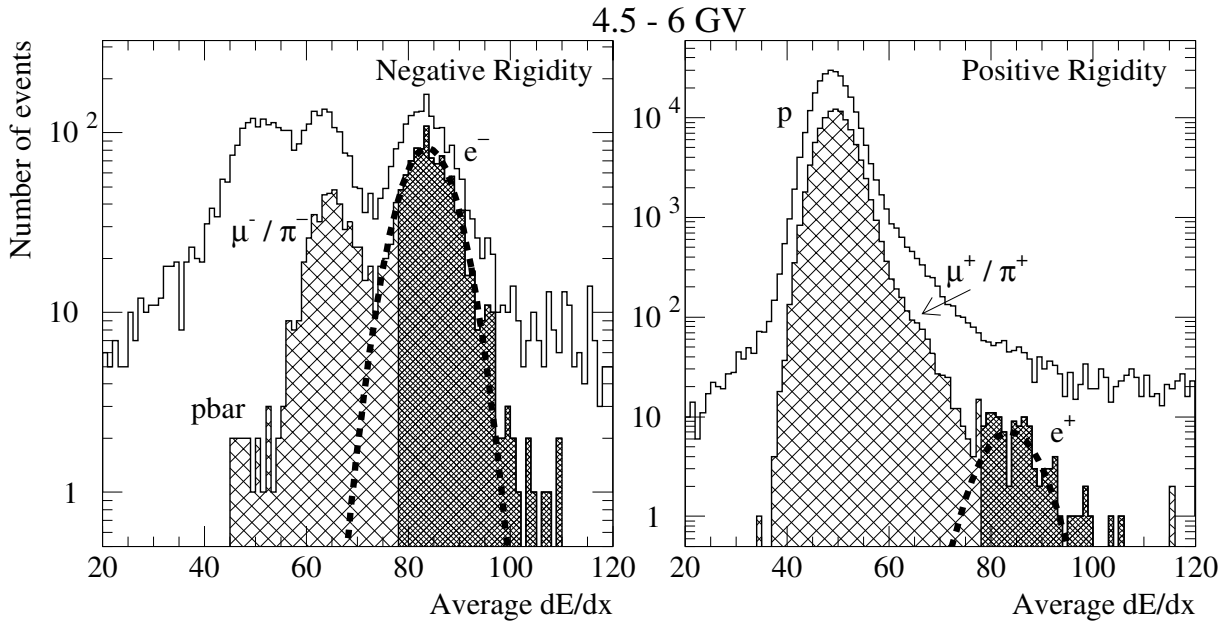


Fig. 1. Distribution of average restricted dE/dx (in arbitrary units) for tracks in the rigidity range 4.5 to 6 GV. The upper distribution is for all events, and the cross-hatched regions are for events having satisfied all selection criteria. The final e^\pm particle counts are from the darker cross-hatched regions.

counters), with a resolution of $\sigma_Z = 0.14$ (in charge units) for each counter. For the present analysis, we reject particles that have a Z within 0.5 of $Z = 2$ in both counters (i.e., within a circle of radius 0.5 centered at (2,2) in $(Z_{top}$ vs. $Z_{bottom})$ space), or particles with a Z larger than 2 in either counter.

The magnet spectrometer measures the sign of the particle's charge from the direction of the deflection in a magnetic field of about 1 T, and the rigidity $R = pc/Ze$ of the particle from the amount of deflection. We retain only events with at least 13 usable tracking points in the magnet's bending plane (out of a total of 17) and at least 6 points in the non-bending plane (out of a total of 8). We also require the hodoscope track χ^2 parameter to satisfy $\chi^2 < 5$. The mean maximum detectable rigidity (MDR, see e.g., Barwick et al. 1997a) achieved is about 160 GV, and we require that all final selected tracks satisfy $|MDR/R| > 4$. The hodoscope track is extrapolated to the top and bottom scintillator locations, and the longitudinal coordinate of the hit is compared with that from the relative timing of the signals at both ends of the paddle. The spatial resolution achieved is 4.6 cm and 5.4 cm for the top and bottom paddles, respectively; we require that the coordinates agree within 10 cm and 15 cm, respectively.

Only the lower 50% of the ionization signals in the 140 chambers (70 above and 70 below the magnet spectrometer) of the multiple dE/dx system are retained to form a restricted average $\langle dE/dx \rangle$ signal. A difference $\Delta \langle dE/dx \rangle$ between the average signals above and below the spectrometer is constructed, and we find agreement with a resolution of $0.14 \langle dE/dx \rangle$; we require $|\Delta \langle dE/dx \rangle| < 0.5 \langle dE/dx \rangle$. Finally, e^\pm induced events tend to result in a greater number

of hits in the ionization chambers of the dE/dx system than heavier singly charged particles, owing to higher electromagnetic energy losses. We require a minimum of 155 total hits in the entire dE/dx stack. Moreover, we require that the total number of chambers used in calculating the restricted average dE/dx be greater than 64 (after the larger 50% of the signals have been rejected).

An example of distributions of $\langle dE/dx \rangle$ for particle tracks having satisfied all the criteria above is shown in Fig. 1, for the rigidity range 4.5 to 6 GV. The upper distribution is for all events, whereas the cross-hatched regions are for events having satisfied all selection criteria. Clearly seen are contributions due to protons (or antiprotons), pions and muons together, and positrons (or electrons). Each distribution is fitted with a sum of 3 Gaussian functions, where the mean and standard deviations are forced to be the same for both the positive and negative rigidity distributions. An example of the best fit for the e^\pm populations is shown as the dashed curve on Fig. 1. Note that the selection criteria employed here were tuned to optimize the identification and statistical significance of the e^\pm peaks, and therefore differ from those employed in the antiproton analysis of Nutter et al. 2001. We obtained similar distributions in the rigidity ranges 6-8.9 GV and 8.9-14.8 GV, but at rigidities above 14.8 GV the small positron contribution cannot be distinguished from that of μ^+/π^+ .

3 Atmospheric Corrections

The atmospheric overburden during the 2000 flight varied between 4.5 and 11 g/cm^2 , for an average overburden of

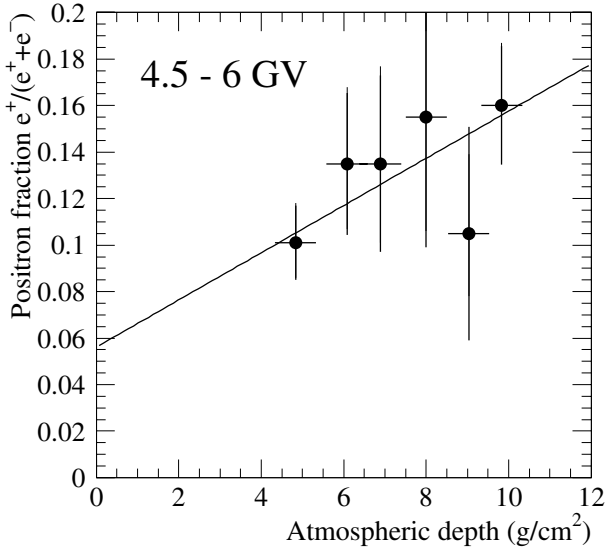


Fig. 2. Positron fraction as a function of atmospheric overburden at rigidities between 4.5 and 6 GV.

7.2 g/cm², which resulted in significant numbers of atmospheric secondaries. This is readily apparent when an atmospheric growth curve is obtained with the following procedure. e^\pm are defined (only for the purpose of determining a growth curve here) as satisfying $85 < \langle dE/dx \rangle < 105$ (in arbitrary units). The data in Fig. 1 are divided into six equal atmospheric depths between 4.5 and 10.5 g/cm², and the electron and positron counts satisfying the above condition are tallied. The resulting positron fraction is then determined in each atmospheric slice, and is plotted for rigidities between 4.5 and 6 GV in Fig. 2. A linear fit is made and shown on the figure, which extrapolates to the top of the atmosphere to a positron fraction of 0.056 ± 0.038 . This procedure results in unacceptably large errors, so that we resort instead to a Monte Carlo calculation of atmospheric secondary production, as described in detail elsewhere (Barwick et al. 1998). The corrections for the positrons vary between 44% and 52%, and those for the electrons between 5.2% and 6.3%. Uncertainties in these atmospheric corrections result in a systematic uncertainty of about ± 0.01 on the positron fraction.

Finally, a correction factor of 1.109 is applied to rigidities at the instrument, to account in an average way for radiative energy losses by the electrons and positrons, and to correct to the top of the atmosphere. This factor is calculated (Barwick et al. 1998) as $\alpha^{t/\alpha \ln 2}$ where t is the average atmospheric depth (expressed in radiation lengths) and $\alpha = 3.1$ is taken for the spectral index of the primary electrons.

4 Results and Discussion

The raw e^\pm particle counts were obtained by tallying the events with a restricted average dE/dx signal greater than

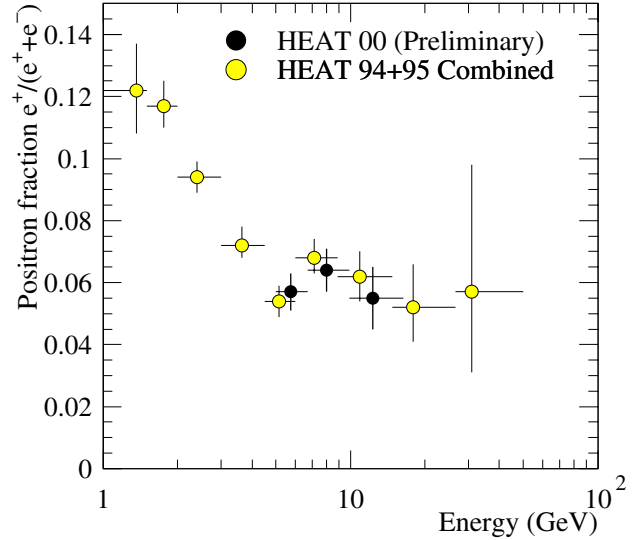


Fig. 3. Positron fraction as a function of energy measured here with the HEAT-pbar instrument, compared to previous HEAT- e^\pm measurements.

one Gaussian standard deviation below the peak of the fitted curve, as illustrated by the darker cross-hatched regions of Fig. 1 (in the 8.9-14.8 GV rigidity range, due to the increased dE/dx losses of pions and muons, we tallied events with an average dE/dx signal greater than that corresponding to the peak of the Gaussian fit only). These counts are summarized in Table 1. They are then corrected for the atmospheric secondaries, and the positron fractions calculated as summarized in Table 1. Note that the positron fraction of 0.057 ± 0.006 at 5-6.7 GeV (ToA) is compatible with the value 0.056 ± 0.038 obtained from the growth curve of Fig. 2. Fig. 3 shows the final corrected positron fractions as a function of energy, compared with the previous combined HEAT- e^\pm results (Barwick et al. 1997) from the 1994 and 1995 flights. The results should be regarded as preliminary pending further refinements in our atmospheric background corrections

Table 1. Compilation of e^\pm results.

Energy (GeV)	e^+		e^-		$e^+/(e^++e^-)$
	Meas./Corr.	Meas./Corr.	Meas./Corr.	Meas./Corr.	
5.0-6.7 (5.73)	106/52.5	933/874	0.057±0.006		
6.7-9.9 (8.00)	87/48.4	744/703	0.064±0.007		
9.9-16.4 (12.27)	35/16.8	302/286	0.055±0.010		

The HEAT-pbar positron fractions reported here are compatible with the previous HEAT- e^\pm measurements obtained with a very different technique. In particular, the new results are consistent with the small feature we observed previously near 7-10 GeV (Coutu et al. 1999).

Acknowledgements. We thank the NSBF balloon crews that have supported the HEAT flights. This work was supported by NASA grants NAG5-5220, NAG5-5223, NAG5-5230 and NAG5-5058, and by financial assistance from our universities.

References

- Agrinier, B. et al. 1969 , Lett. Nuovo Cimento, 1, 153.
Barbiellini, G. et al. 1996, A&A, 309, L15.
Barwick, S. W. et al. 1995, Phys. Rev. Lett., 75, 360.
Barwick, S. W. et al. 1997, ApJ, 482, L191.
Barwick, S. W. et al. 1997, Nucl. Inst. & Meth. A, 400, 34.
Barwick, S. W. et al. 1998, ApJ, 498, 779.
Buffington, A. et al. 1975, ApJ, 199, 669.
Clem, J. M. et al. 1996, ApJ, 464, 507.
Coutu, S. et al. 1999, Astropart. Phys. 11, 427.
Golden, R. L. et al. 1987, A&A, 188 145.
Golden, R. L. et al. 1994, ApJ, 436, 769.
Golden, R. L. et al. 1996, ApJ, 457, L103.
Kamionkowski, M. & Turner, M. S. 1991, Phys. Rev. D, 43, 1774.
Moskalenko, I. V. & Strong, A. W. 1998, ApJ 493, 694.
Müller, D. & Tang, K. 1987, ApJ, 312, 183.
Musser, J. et al. 2001, these proceedings.
Nutter, S. et al. 2001, these proceedings.
Protheroe, R. J. 1982, ApJ, 254, 391.